BIOCHEMISTRY
including biophysical chemistry & molecular biology

Article

pubs.acs.org/biochemistry

Characterization of the Side-Chain Hydroxyl Moieties of Residues Y56, Y111, Y238, Y338, and S339 as Determinants of Specificity in *E. coli* Cystathionine β-Lyase

Pratik H. Lodha and Susan M. Aitken*

Department of Biology, Carleton University, Ottawa, Canada K1S 5B6

ABSTRACT: Cystathionine β-lyase (CBL) catalyzes the hydrolysis of L-cystathionine (L-Cth) to produce L-homocysteine, pyruvate, and ammonia. A series of site-directed variants of *Escherichia coli* CBL (eCBL) was constructed to investigate the roles of the hydroxyl moieties of active-site residues Y56, Y111, Y238, Y338, and S339 as determinants of specificity. The effect of these conservative substitutions on the $k_{cat}/K_m^{L\text{-}Cth}$ for the α,β-elimination of L-Cth ranges from a change of only 1.1-fold for Y338F to a reduction of 3 orders of magnitude for the alanine replacement variant of S339. A novel role for residue S339 as a determinant of reaction specificity, via tethering of the catalytic base, K210, is demonstrated. Comparison of the kinetic parameters for L-Cth hydrolysis with those for the inhibition of eCBL by aminoethoxyvinylglycine (AVG) indicates that Y238 interacts with the distal carboxylate group of the substrate. The 22 and 50-fold increases in the $K_m^{L\text{-}Cth}$ and K_i^{AVG} resulting from replacement of Y56 with phenylalanine suggest that this residue may interact with the distal amino group of these compounds, although an indirect role in binding is more likely. The near-native $k_{cat}/K_m^{L\text{-}Cth}$ and pH profile of the eCBL-Y111F variant demonstrate that residue Y111 does not play a role in proton transfer. The understanding of the eCBL active site and of the determinants of substrate and reaction specificity resulting from this work will facilitate the design of inhibitors, as antibacterial therapeutics, and the engineering of enzymes dependent on the catalytically versatile pyridoxal 5′-phosphate cofactor to modify reaction specificity.

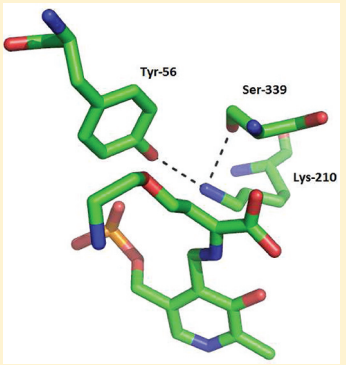

The transsulfuration pathway converts L-cysteine (L-Cys), synthesized de novo by bacteria and plants, to L-homocysteine (L-Hcys), the precursor of L-methionine (L-Met). The L-cystathionine (L-Cth) product of cystathionine γ-synthase (CGS) is cleaved by cystathionine β-lyase (CBL), the second enzyme of the transsulfuration pathway, via an α,β-elimination reaction, to produce L-Hcys, pyruvate, and ammonia (Scheme 1). In contrast, cystathionine γ-lyase (CGL), which follows cystathionine β-synthase (CBS) in the reverse transsulfuration pathway of mammals and *Saccharomyces cerevisiae*, catalyzes the hydrolysis of L-Cth, via an α,γ-elimination reaction, to yield L-Cys, α-ketobutyrate, and ammonia.[1,2] The enzymes CGS and CBL are targets for the development of herbicides and antimicrobial compounds because the transsulfuration pathway is unique to bacteria and plants.[3−5]

Phylogenetic analysis has demonstrated that there are five structurally distinct families, or fold types, of pyridoxal 5′-phosphate (PLP)-dependent enzymes.[6] With the exception of CBS, which is a member of fold-type II, the enzymes of the transsulfuration and reverse transsulfuration pathways are members of the γ-subfamily of fold-type I. The striking structural similarity of the γ-subfamily is illustrated by the ∼1.5-Å rms deviation in the least-squares superposition of ∼350 C_α atoms of the protein backbones of *Escherichia coli* CGS (eCGS), *E. coli* CBL (eCBL), *S. cerevisiae* CGL (yCGL), and *Trichomonas vaginalis* methionine γ-lyase (tMGL), which share ∼35% amino acid sequence identity.[4,7−9] The residues lining the active-site cavities are largely conserved among these enzymes, suggesting that substrate and reaction specificity is primarily the result of differences in the placement and mobility of active-site residues. Therefore, the fold-type I enzymes of the transsulfuration pathways provide a useful model system to investigate determinants of specificity, information which will facilitate the engineering of enzymes dependent on the catalytically versatile PLP cofactor.

The structures of eCBL in complex with the inhibitors aminoethoxyvinylglycine (AVG), *N*-hydrazinocarbonylmethyl-2-nitrobenzamide, and *N*-hydrazinocarbonylmethyl-2-trifluoromethylbenzamide provide valuable insight into both the contacts of the L-Cth substrate in the active site and the mechanism of this enzyme (Scheme 1).[3,5] Lodha et al. confirmed the interactions between the α-carboxylate groups of L-Cth and AVG and the side chains of residues W340 and R372, observed in the structure of the eCBL−AVG complex, and identified R58 as the residue which binds the distal carboxylate moiety of L-Cth, not present in AVG (Scheme 2).[3,10] There are four active-site tyrosines (Y56, Y111, Y238, and Y338) and a serine (S339) residue that are conserved in bacterial CBL sequences (Scheme 2). Residues Y56, Y111, and S339 are also conserved in eCGS and yCGL, while Y238 and Y338 are replaced by asparagine and glutamate, respectively, in

Received: July 13, 2011
Revised: September 25, 2011
Published: September 29, 2011

Scheme 1. (A) DTNB and LDH Assays Employed to Measure the L-Cth Activity of eCBL. (B) Structures of L-Cth and the Related Compounds L-Cys, OAS, and L-Lanthionine and the Slow-Binding Inhibitors of eCBL: AVG, *N*-Hydrazinocarbonylmethyl-2-nitrobenzamide, and *N*-Hydrazinocarbonylmethyl-2-trifluoromethylbenzamide[3,5]

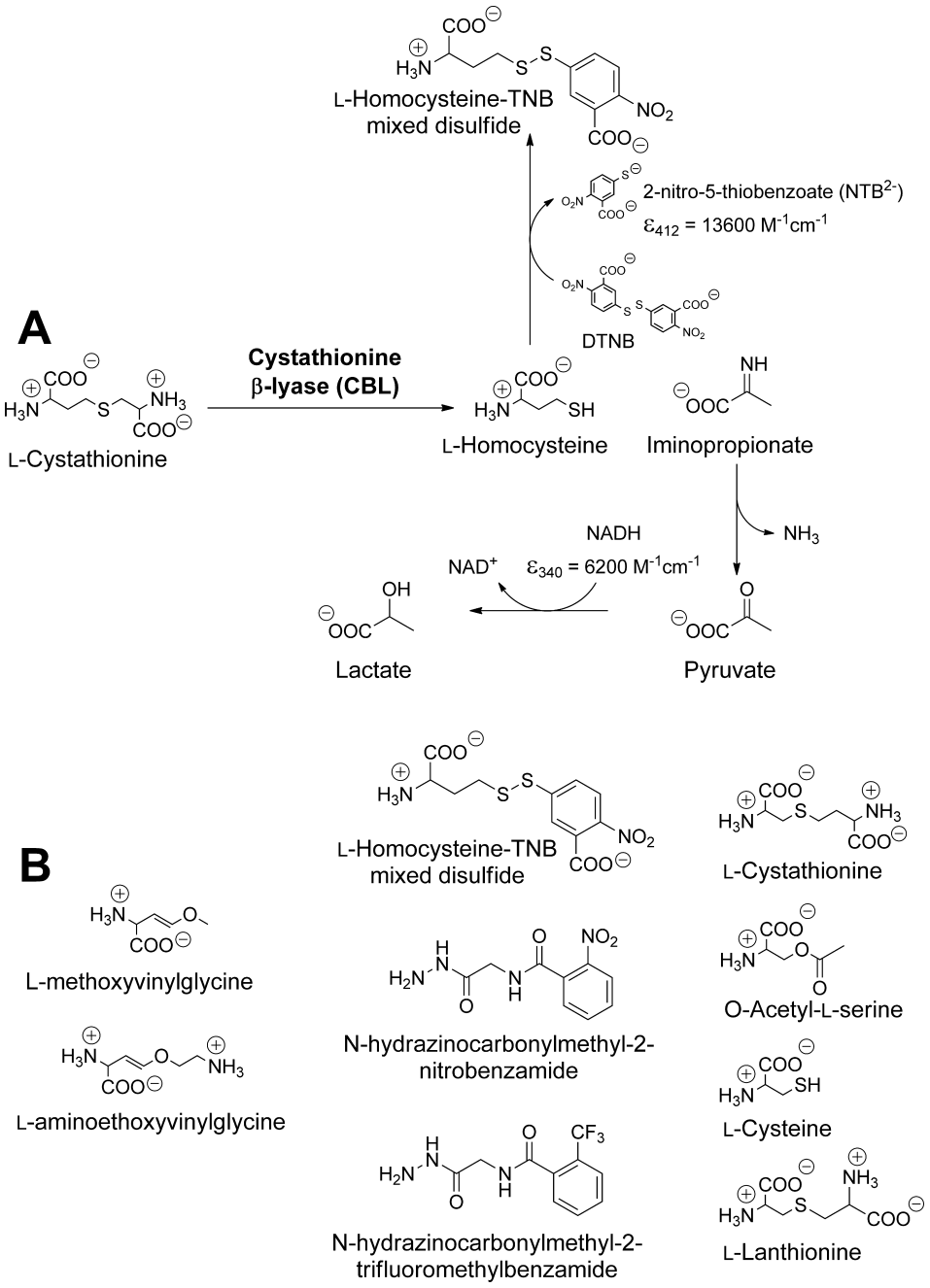

these enzymes. The side chains of Y111, Y238, and Y338 of eCBL have been proposed to interact with the L-Cth substrate of eCBL.[4,7,9] A series of site-directed variants, removing only the side-chain hydroxyl groups, of residues Y56, Y111, Y238, Y338, and S339 was constructed to investigate the roles of the hydrogen bonding interactions of these side chains (Scheme 2).

MATERIALS AND METHODS

Reagents. *O*-Acetyl-L-serine (OAS), L-aminoethoxyvinylglycine (AVG), L-Cth [*S*-(2-amino-2-carboxyethyl)-L-homocysteine], L-Cys, L-lactate dehydrogenase (LDH), *β*-nicotinamide adenine dinucleotide (*β*-NADH, reduced form), and L-Ser were purchased from Sigma. Ni-NTA resin and 5,5′-dithiobis(2-nitrobenzoic acid) (DTNB) were obtained from Qiagen and Pierce, respectively. Oligonucleotide primers were synthesized by Integrated DNA Technologies, and site-directed mutants were sequenced by BioBasic prior to expression and purification.

Construction, Expression, and Purification of Site-Directed Mutants. Site-directed mutants of eCBL were constructed, expressed, and purified as described by Farsi et al.[11] The *E. coli* KS1000 *metC::cat* strain, in which the gene encoding eCBL is replaced with chloramphenicol acetyltransferase, was employed for expression to avoid contamination with the wild-type *E. coli* enzyme.[11] The presence of the N-terminal, 6-His tag, and linker, encoded by the pTrc-99aAF

dx.doi.org/10.1021/bi201090n | *Biochemistry* 2011, 50, 9876–9885

Scheme 2. Observed Contacts of the PLP-AVG External Aldimine Active Site of eCBL[a]

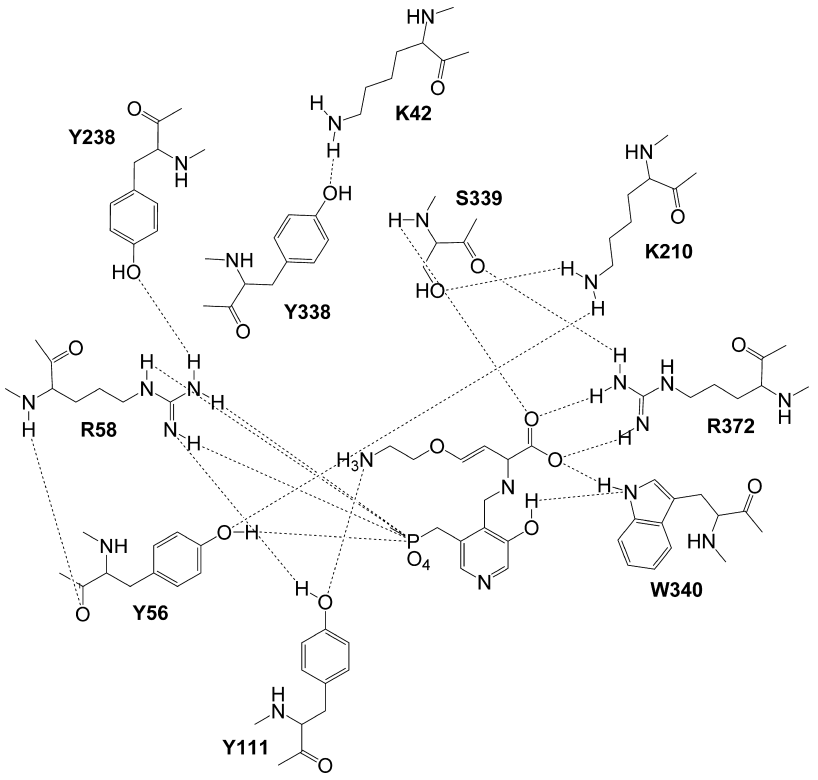

[a]The dotted lines represent putative hydrogen bond distances of ≤3.3 Å between heteroatoms. The image was constructed using ChemDraw and PDB entry 1CL2.[3].

expression vector, does not alter the kinetic properties of eCBL.[11]

Determination of Steady-State Kinetic Parameters. Enzyme activity was measured using a Spectramax 340 microtiter plate spectrophotometer (Molecular Devices) in a total volume of 100 μL at 25 °C. The assay buffer was composed of 50 mM Tris, pH 8.5, containing 20 μM PLP. The hydrolysis of L-Cth (0.01−6.25 mM) was detected via the reaction of 5,5′-dithiobis-(2-nitrobenzoic acid) (DTNB) with the free thiol of the L-Hcys product (ε_{412} = 13600 M^{-1} s^{-1}) and by using the coupling enzyme L-lactate dehydrogenase (LDH), which reduces the pyruvate product to lactate, with the concomitant conversion of NADH to NAD^+ (ε_{340} = 6200 M^{-1} s^{-1}) (Scheme 1).[11−13] The LDH assay was also employed to monitor the hydrolysis of OAS and L-Cys. A background reading was recorded before initiation of the reaction by the addition of eCBL (0.02−10.3 μM for DTNB assay or 0.12−16.2 μM for LDH assay, depending on the activity of the enzyme variant). Values of k_{cat} and K_m for the hydrolysis of L-Cth and OAS were obtained by fitting of the data to the Michaelis−Menten equation, and k_{cat}/K_m was obtained independently from eq 1. The L-Cys hydrolysis data was fit to eq 2, which incorporates the $K_i^{L\text{-}Cys}$ term for substrate inhibition by L-Cys, and $k_{cat}/K_m^{L\text{-}Cys}$ was obtained independently from eq 3. Data were fit by nonlinear regression with the SAS software package (SAS Institute, Cary, NC).

$$\frac{v}{[E]} = \frac{\frac{k_{cat}}{K_m} \times [S]}{1 + \frac{[S]}{K_m}} \quad (1)$$

$$\frac{v}{[E]} = \frac{k_{cat} \times [S]}{K_m^{L-Cys} + [S]\left(1 + \frac{[S]}{K_i^{L-Cys}}\right)} \quad (2)$$

$$\frac{v}{[E]} = \frac{\frac{k_{cat}}{K_m} \times [S]}{1 + \frac{[S]}{K_m}\left(1 + \frac{[S]}{K_i^{L-Cys}}\right)} \quad (3)$$

Evaluation of the pH Dependence of Wild-Type and Site-Directed Variants of eCBL. The pH dependence of L-Cth hydrolysis by eCBL was determined using the continuous DTNB and LDH assays in a three-component buffer, composed of 50 mM MOPS (pK_a = 7.2), 50 mM Bicine (pK_a = 8.3), and 50 mM proline (pK_a = 10.7).[14,15] The kinetic measurements were carried out between pH 6.4−10.6 in the presence of 20 μM PLP, 0.06−3.0 μM eCBL (depending on the activity of the site-directed variant), and 6.25 mM L-Cth, for specific activity measurements, or 0.01−6.25 mM L-Cth, for the determination of $k_{cat}/K_m^{L\text{-}Cth}$. Specific activity versus pH measurements were performed at least in triplicate. The $k_{cat}/K_m^{L\text{-}Cth}$ versus pH data were fit to the bell-shaped curve described by eq 4, where k_{cat}/K_m^{max} is the upper limit for $k_{cat}/K_m^{L\text{-}Cth}$ at the pH optimum.[13]

$$\frac{k_{cat}}{K_m} = \frac{\frac{k_{cat}}{K_m^{max}}}{1 + 10^{pK_{a1} - pH} + 10^{pH - pK_{a2}}} \quad (4)$$

Inhibition of Wild-Type and Site-Directed Variants of eCBL by AVG. The IC_{50}^{AVG} values for inhibition of the eCBL

Table 1. Kinetic Parameters for L-Cth Hydrolysis and Inhibition by AVG of eCBL and Site-Directed Variants

enzyme	assay	k_{cat}[a] (s^{-1})	$K_m^{L\text{-}Cth}$[a] (mM)	$k_{cat}/K_m^{L\text{-}Cth}$[a] ($M^{-1}\,s^{-1}$)	IC_{50}^{AVG}[b] (μM)	K_i^{AVG}[c] (μM)	k_2[c] (s^{-1})
eCBL	DTNB	34.1 ± 0.6	0.18 ± 0.01	(1.9 ± 0.1) × 10^5	1.74 ± 0.08	1.9 ± 0.6	(5 ± 1) × 10^{-4}
	LDH	28.3 ± 0.2	0.188 ± 0.007	(1.50 ± 0.05) × 10^5	2.8 ± 0.3	3 ± 2	(6 ± 3) × 10^{-4}
Y56F	DTNB	10.4 ± 0.6	18 ± 1	(5.82 ± 0.09) × 10^2	23 ± 1	188 ± 9	(2.5 ± 0.1) × 10^{-3}
	LDH	4.85 ± 0.08	4.1 ± 0.1	(1.18 ± 0.02) × 10^3	140 ± 30	142 ± 5	(2.1 ± 0.1) × 10^{-3}
Y111F	DTNB	n.s.	n.s.	76 ± 1	1.34 ± 0.05	n.d.	n.d.
	LDH	12.4 ± 0.1	0.67 ± 0.02	(1.86 ± 0.04) × 10^4	1.61 ± 0.09	2.7 ± 0.9	(1.3 ± 0.4) × 10^{-3}
Y238F	DTNB	62.3 ± 0.5	4.59 ± 0.07	(1.36 ± 0.01) × 10^4	4.6 ± 0.3	6.9 ± 0.3	(1.9 ± 0.1) × 10^{-3}
	LDH	26.4 ± 0.3	2.88 ± 0.07	(9.2 ± 0.1) × 10^3	5.8 ± 0.5	1.45 ± 0.08	(2.7 ± 0.1) × 10^{-3}
Y338F	DTNB	157 ± 3	0.27 ± 0.02	(6.0 ± 0.5) × 10^5	2.6 ± 0.4	5 ± 2	(2.1 ± 0.1) × 10^{-3}
	LDH	46.9 ± 0.6	0.27 ± 0.01	(1.71 ± 0.07) × 10^5	2.8 ± 0.2	1 ± 1	(2 ± 2) × 10^{-4}
S339A	DTNB	(9.9 ± 0.2) × 10^{-3}	0.11 ± 0.01	92 ± 8	3.3 ± 0.6 ^{DTNB}	2.7 ± 0.8	(2.6 ± 0.8) × 10^{-4}
	LDH	(5.04 ± 0.06) × 10^{-3}	0.087 ± 0.005	58 ± 3	n.d.	n.d.	n.d.

[a]Kinetic parameters reported are for hydrolysis of L-Cth. Reaction conditions: 0.01−6.4 mM, L-Cth, 0.02−10.3 μM (DTNB assay), or 0.12−16.2 μM (LDH assay) wild-type or mutant eCBL (depending on the activity of the enzyme) and 2 mM DTNB to monitor L-Hcys production, or 1.5 mM NADH and 2.0 μM LDH, to monitor pyruvate production, in assay buffer at 25 °C. The data were fit to the Michaelis−Menten equation to obtain k_{cat} and $K_m^{L\text{-}Cth}$ and eq 1 to obtain $k_{cat}/K_m^{L\text{-}Cth}$. The notation n.s. indicates that Y111F does not display saturation kinetics within the solubility limit of the substrate when monitored with the DTNB assay because of inhibition by the latter. [b]Reaction conditions for IC_{50}^{AVG} measurements: Enzyme (0.029−3.6 μM, depending on the activity of the mutant) was incubated with 0.05−10^4 μM AVG in assay buffer at 25 °C for 10 min. Activity was subsequently measured, via the DTNB (n = 4) and LDH-based coupled (n = 3) assays at a L-Cth substrate concentration of 0.1 mM. The data were fit to eq 5 to obtain IC_{50}^{AVG}. The IC_{50}^{AVG} of the S339A variant could not be accurately determined with the LDH assay due to its low activity. [c]Reaction conditions for measurement of K_i^{AVG} and k_2: Wild-type eCBL and site-directed variants (0.023−8.1 μM, depending on the activity of the enzyme) were incubated with 1.5 mM L-Cth and 0.005−7.5 mM AVG in assay buffer, and the progress of the reactions was monitored for 30 min via the DTNB- and LDH-based coupled assays. The progress curves were fit to eq 6 to obtain k_{obs} values, which were plotted versus inhibitor concentration and fit to eq 7 to obtain k_2 and K_i^{AVG}. The K_i^{AVG} and k_2 of the Y111F and S339A variants could not be accurately determined with the DTNB and LDH assays, respectively, because of their low activity.

Table 2. Kinetic Parameters of eCBL and Site-Directed Mutants for the Hydrolysis of OAS and L-Cys[a]

	OAS → acetate + pyruvate + NH_3			L-cysteine → H_2S + pyruvate + NH_3			
enzyme	k_{cat} (s^{-1})	K_m^{OAS} (mM)	k_{cat}/K_m^{OAS} ($M^{-1}s^{-1}$)	k_{cat} (s^{-1})	$K_m^{L\text{-}Cys}$ (mM)	$K_i^{L\text{-}Cys}$ (mM)	$k_{cat}/K_m^{L\text{-}Cys}$ ($M^{-1}s^{-1}$)
eCBL	0.280 ± 0.004	2.18 ± 0.09	128 ± 4	0.49 ± 0.02	0.24 ± 0.02	4.9 ± 0.5	2000 ± 100
Y56F	n.s.	n.s.	0.27 ± 0.02	0.0048 ± 0.0007	0.02 ± 0.01	0.6 ± 0.2	230 ± 80
R58A	0.57 ± 0.07	51 ± 8	11.2 ± 0.4	0.173 ± 0.007	0.36 ± 0.04	13 ± 2	480 ± 40
Y111F	0.0131 ± 0.0007	13 ± 1	0.98 ± 0.05	0.17 ± 0.02	0.11 ± 0.02	0.65 ± 0.09	1500 ± 100
Y238F	0.250 ± 0.005	3.1 ± 0.2	81 ± 3	0.55 ± 0.03	0.46 ± 0.06	10 ± 1	1200 ± 100
Y338F	0.515 ± 0.006	2.79 ± 0.09	185 ± 4	0.39 ± 0.02	0.23 ± 0.03	4.2 ± 0.6	1700 ± 200

[a]Kinetic parameters reported are for hydrolysis of OAS and L-Cys. The activity of S339A for the hydrolysis of L-Cys and OAS is undetectable. Reaction conditions: 1.5 mM NADH, 2.0 μM LDH, 0.01−20 mM OAS or L-Cys, and 2.6−7.7 μM eCBL enzyme, depending on the activity of the variant, in assay buffer at 25 °C. The OAS data were fit to the Michaelis−Menten equation to obtain k_{cat} and K_m^{OAS} and eq 1 to obtain k_{cat}/K_m^{OAS} and the L-Cys data were fit to eq 2 to obtain k_{cat} and $K_m^{L\text{-}Cys}$ and eq 3 to obtain $k_{cat}/K_m^{L\text{-}Cys}$. The notation n.s. indicates that Y56F does not display saturation kinetics within the solubility limit of the OAS substrate.

enzymes by AVG were determined by measuring enzyme activity between 5 × 10^{-5} and 10 mM AVG. The enzyme and inhibitor were mixed and incubated at 25 °C for 10 min in assay buffer. Activity was subsequently measured at a L-Cth substrate concentration of 0.1 mM, and the data were fit to eq 5.[5] Measurements were performed in quadruplicate for each enzyme. The parameters Act_{max}, Act_{min}, S, and IC_{50}^{AVG} of eq 5 correspond to the maximal enzyme activity, the minimal enzyme activity, the slope of the transition between the maximal and minimal activity plateaus, and the midpoint of the transition, respectively.

$$Act = \frac{Act_{max} - Act_{min}}{1 + \left(\frac{I}{IC_{50}}\right)^{S}} + Act_{min} \quad (5)$$

Values for the dissociation constant K_i^{AVG} and the rate constant k_2 for the inhibition of eCBL by AVG were determined using the model described by Clausen et al. in which formation of the enzyme−inhibitor complex is slow.[3] The wild-type eCBL and site-directed variant enzymes were incubated with 1.5 mM L-Cth and 0.005−7.5 mM AVG in assay buffer and the progress of the reactions was monitored for 30 min. Values of k_{obs} were determined from the fit of eq 6 to the progress curves. The resulting k_{obs} values were plotted versus inhibitor concentration and values of k_2 and K_i^{AVG} were obtained by fitting the data to eq 7. The K_i^{AVG} and k_2 of eCBL-S339A could not be accurately determined with the LDH assay because of its low activity.

$$[P] = v_s t + \frac{(v_o - v_s)[1 - \exp^{-k_{obs}t}]}{k_{obs}} \quad (6)$$

$$k_{obs} = k_2 + \frac{k_2[I]}{K_i\left(1 + \frac{[S]}{K_m}\right)} \quad (7)$$

dx.doi.org/10.1021/bi201090n | Biochemistry 2011, 50, 9876−9885

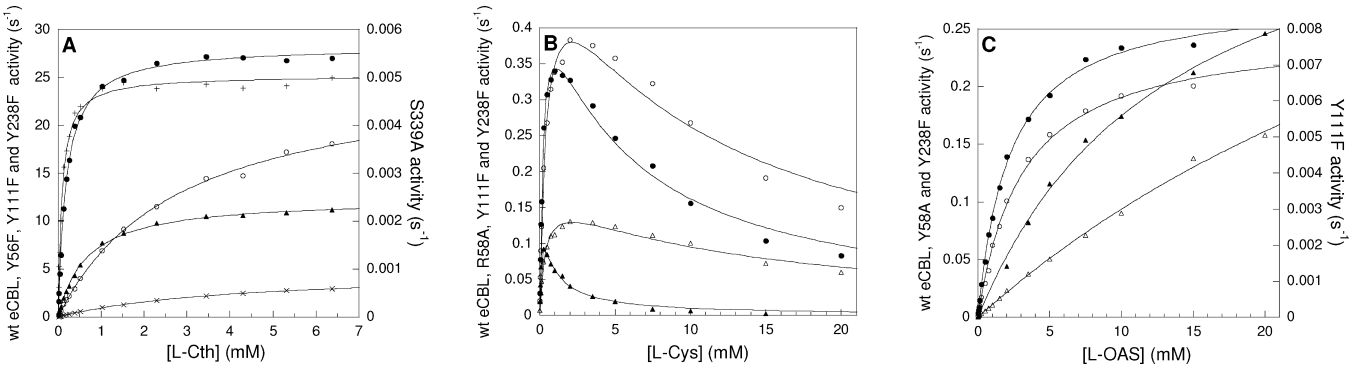

Figure 1. Dependence of (A) Wt-eCBL (●), Y56F (×), Y111F (▲), Y238F (○), and S339A (+); (B) Wt-eCBL (●), R58A (Δ), Y111F (▲), and Y238F (○); and (C) Wt-eCBL (●), R58A(Δ), Y111F (▲), and Y238F (○) activity on the concentration of (A) L-Cth, (B) L-Cys, and (C) L-OAS.

RESULTS

The five phenylalanine and alanine substitution variants were soluble with yields between 17 and 40 mg/L, which is similar to the 15−41 and 56 mg/L values reported for a series of arginine replacement variants of eCBL and the wild-type enzyme, respectively.[10,11] The L-Cth-hydrolysis activity of the eCBL variants was measured with both the DTNB and LDH assays, which monitor production of the L-Hcys and pyruvate products, respectively (Scheme 1). The kinetic parameters determined with the two assays are within ~2-fold for all enzymes except Y111F, which is sensitive to the presence of DTNB. The values for both assays are presented in Table 1, and unless otherwise stated, the kinetic parameters of L-Cth hydrolysis and inhibition by AVG described in the text were determined with the LDH assay. The ability of each enzyme to catalyze the hydrolysis of OAS and L-Cys was also investigated to probe the role of the targeted residues as determinants of substrate specificity. The specific activity of L-Cth hydrolysis and the $k_{cat}/K_m^{L\text{-}Cth}$ versus pH profiles of the wild-type enzyme and the five site-directed variants are bell-shaped.

The Y56F Variant. The k_{cat} and $K_m^{L\text{-}Cth}$ values, for L-Cth hydrolysis, of eCBL-Y56F are decreased 5.8-fold and increased 22-fold, respectively, resulting in a 130-fold decrease in catalytic efficiency (Table 1). The OAS-hydrolysis data of the Y56F variant could not be fit to the Michaelis−Menten equation, as saturation kinetics were not observed. Therefore, with the assumption that $K_m^{OAS} \gg$ [L-OAS], the Michaelis−Menten equation was modified to obtain k_{cat}/K_m^{OAS}, which is reduced 470-fold compared to the wild-type enzyme (Table 2). In contrast, the k_{cat}, $K_m^{L\text{-}Cys}$, $K_i^{L\text{-}Cys}$, and $k_{cat}/K_m^{L\text{-}Cys}$, for L-Cys hydrolysis, of Y56F are all reduced, by 100-, 12-, 8-, and 9-fold, respectively (Table 2, Figure 1), while the IC_{50}^{AVG} and K_i^{AVG} values for inhibition of Y56F by AVG are both increased 50-fold (Table 1), compared to the wild-type enzyme. Substitution of Y56 with phenylalanine results in a shift in the acidic limb of the specific activity versus pH profile. The pH optimum of eCBL−Y56F is correspondingly shifted to 9−9.5, compared to 8.5−9 for the wild-type enzyme. Therefore, the effect of pH on the $k_{cat}/K_m^{L\text{-}Cth}$ of Y56F was determined (Figure 2). The values of pK_{a1} and pK_{a2} of the wild-type enzyme, corresponding to the acidic and basic limbs of the $k_{cat}/K_m^{L\text{-}Cth}$ versus pH profile, respectively, are 8.0 ± 0.1 and 10.1 ± 0.1, while those of the Y56F variant are 8.7 ± 0.1 and 10.1 ± 0.1, respectively (Table 3). The pK_{a1} value of Y56F is consistently increased 0.7 pH units when measured with either assay.

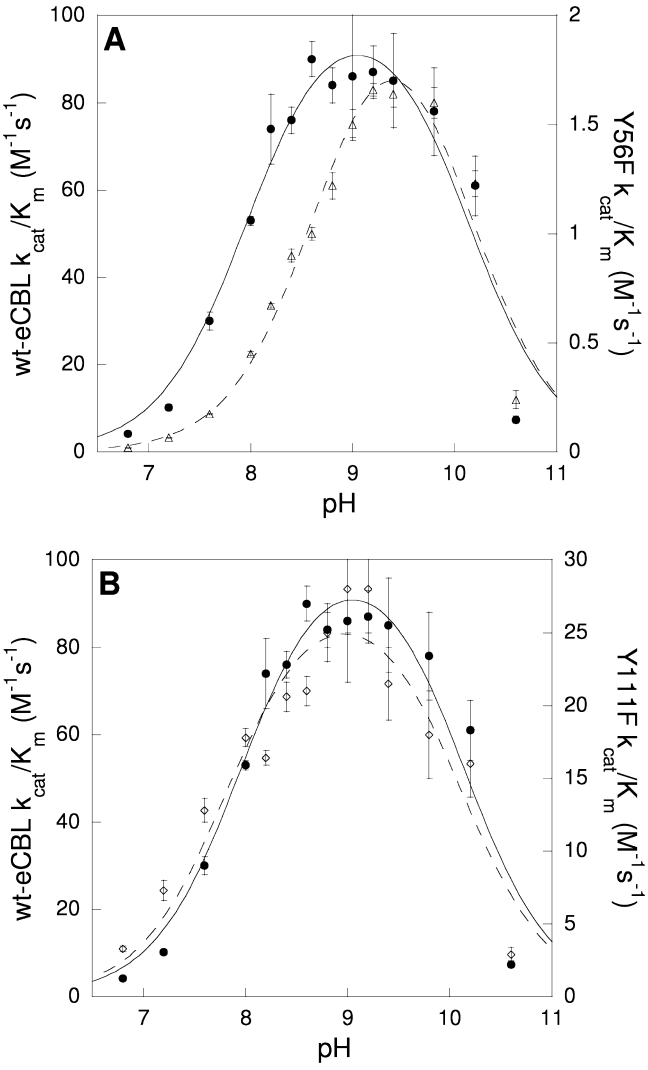

Figure 2. Comparison of the pH dependence of $k_{cat}/K_m^{L\text{-}Cth}$ for L-Cth hydrolysis by wild-type eCBL (●, solid line) and the (A) Y56F (Δ, dashed line) and (B) Y111F (◇, dashed line) variants. Reaction conditions: MBP buffer (50 mM MOPS, 50 mM bicine, and 50 mM proline), 20 μM PLP, 1.25 mM NADH, 1−6 μM LDH (concentration optimized for each pH), 0.05−6.6 mM L-Cth and 0.11 wild-type eCBL, 0.93 μM Y11F, or 7.9 μM S339A. The data were fit to eq 4.

The Y111F Variant. The k_{cat} and $K_m^{L\text{-}Cth}$ of Y111F are decreased 2.3-fold and increased 3.6-fold, respectively (Table

dx.doi.org/10.1021/bi201090n | Biochemistry 2011, 50, 9876−9885

Table 3. Parameters Determined from the $k_{cat}/K_m^{L\text{-}Cth}$ versus pH Profiles of Wild-Type eCBL and the Y56F and Y111F Variants[a]

enzyme	Assay	pK_{a1}	pK_{a2}
eCBL	DTNB	8.28 ± 0.06	10.20 ± 0.06
	LDH	8.0 ± 0.1	10.1 ± 0.1
Y56F	DTNB	9.01 ± 0.07	10.43 ± 0.09
	LDH	8.7 ± 0.1	10.1 ± 0.1
Y111F	DTNB	7.8 ± 0.3	9.7 ± 0.3
	LDH	7.8 ± 0.1	10.1 ± 0.1

[a]Kinetic measurements for the eCBL-catalyzed hydrolysis of L-Cth were carried out from pH 6.4−10.6 in MBP buffer containing 0.05−6.6 mM L-Cth, 20 μM PLP, 0.03−5.75 μM enzyme, and 2 mM DTNB or 1.25 mM NADH and 1−6 μM LDH (concentration optimized for each pH) at 25 °C. The $k_{cat}/K_m^{L\text{-}Cth}$ versus pH data were fitted to eq 4 to obtain the values for pK_{a1} and pK_{a2}.

1). A unique feature of the Y111F variant is the difference in L-Cth hydrolysis activity observed with the LDH and DTNB assays, which measure the production of pyruvate and L-Hcys, respectively. Figure 3 shows that when pyruvate production is

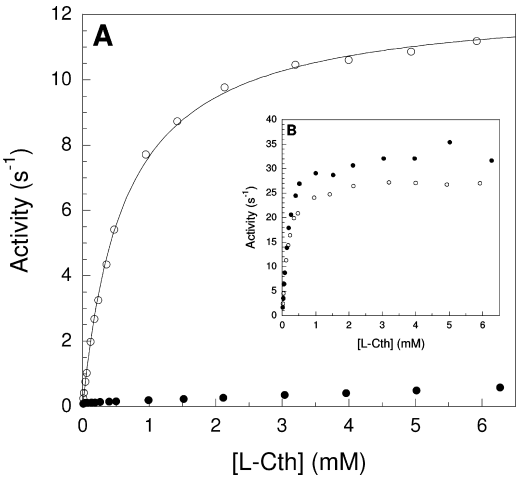

Figure 3. Comparison of the dependence of (A) Y111F and (B) wild-type eCBL activity on the concentration of L-Cth when measured with the DTNB (●) and LDH (○) assays. Reaction conditions: 50 mM Tris, pH 8.5, 20 μM PLP, 0.01−6.3 mM L-Cth, 0.05 μM eCBL or 2.5 μM Y111F, for the DNTB assay, or 0.1 μM eCBL or 0.9 μM Y111F, for the LDH assay, and either 2 mM DTNB or 1.3 mM NADH and 1.9 μM LDH.

measured Y111F displays saturation kinetics, similar to the wild-type enzyme, while in the presence of DTNB the activity is reduced 20-fold at 6.27 mM L-Cth, the highest substrate concentration tested, and the enzyme is not saturated within the solubility limit of L-Cth. The L-Hcys formed upon hydrolysis of L-Cth reacts with DTNB to release TNB^- and produce the mixed disulfide of TNB and L-Hcys (TNB-Hcys), which is similar in overall structural form to *N*-hydrazinocarbonylmethyl-2-nitrobenzamide (Scheme 1), an eCBL inhibitor with an IC_{50} of 4.5 μM.[5] However, up to 100 μM TNB-Hcys, synthesized by reaction of equimolar L-Hcys and DTNB, has no effect on the activity of the wild-type enzyme and Y111F variant. In contrast, addition of DTNB at a concentration as low as 3 μM results in a prolonged lag period prior to detection of pyruvate production when the L-Cth hydrolysis of Y111F, but not the wild-type enzyme, is monitored via the LDH assay. Although the Y111F substitution reduces the $k_{cat}/K_m^{L\text{-}Cys}$, for the α,β-elimination of L-Cys, by only 1.3-fold, the $K_i^{L\text{-}Cys}$ for substrate inhibition is decreased 7.5-fold (Figure 1B, Table 2), indicating that removal of the hydroxyl group of Y111 facilitates the binding of a second molecule of L-Cys to the eCBL active site. The Y111F substitution has no effect on the specific activity, k_{cat} and $k_{cat}/K_m^{L\text{-}Cth}$ versus pH profiles of eCBL (Figure 2). The pK_{a1} and pK_{a2} values of the $k_{cat}/K_m^{L\text{-}Cth}$ profile of the Y111F variant, measured with the LDH assay, are 7.8 ± 0.1 and 10.1 ± 0.1, which is within experimental error of the wild-type enzyme (Table 3).

The Y238F Variant. The k_{cat} of Y238F is identical to the wild-type enzyme (Table 1) and the specific activity and $k_{cat}/K_m^{L\text{-}Cth}$ versus pH profiles of this variant are unchanged. Although the $K_m^{L\text{-}Cth}$, for hydrolysis of L-Cth, of Y238F is increased 15-fold, the IC_{50}^{AVG} and K_i^{AVG} values, for inhibition by by AVG, and the values of K_m^{OAS} and $K_m^{L\text{-}Cys}$, for hydrolysis of OAS and L-Cys, respectively, are increased by only 2−2.5-fold (Tables 1 and 2). The distal carboxylate of L-Cth, the physiological substrate of eCBL, distinguishes it from AVG, OAS and L-Cys, which each possess a single α-carboxylate group. The substrate inhibition observed for wild-type eCBL, in the α,β-elimination of L-Cys, is reduced in the Y238F and R58A variants by 2 and 2.7-fold, respectively, supporting a role for both residues in binding the α-carboxylate group of the second L-Cys molecule, occupying the binding site of the distal portion of the physiological L- Cth substrate (Figure 1B, Table 2).

The Y338F Variant. The effect of substitution of Y338 with phenylalanine is negligible, as the steady-state kinetic parameters for L-Cth, OAS, and L-Cys hydrolysis and the IC_{50}^{AVG} and K_i^{AVG} values, for inhibition by AVG, are all within 2-fold of the corresponding values for the wild-type eCBL enzyme (Tables 1 and 2). The pH profile and optimum of eCBL are also unchanged by the Y338F substitution.

The S339A Variant. The 2600-fold decrease in the $k_{cat}/K_m^{L\text{-}Cth}$ of S339A is dominated by a 5600-fold decrease in k_{cat}. This reduction in k_{cat}, by 3 orders of magnitude, distinguishes S339A as the other active-site variants investigated altered this parameter by only 1.1−5.8-fold (Table 1, Figure 1). The K_i^{AVG} is increased by 2.2-fold and the IC_{50}^{AVG} for inhibition by AVG, which could be measured with only the DTNB assay due to the low activity of this variant, was also increased by only ∼2-fold. The low activity of the S339A variant precluded the measurement of OAS and L-Cys hydrolysis, as the k_{cat} of the wild-type enzyme for these substrates is 2 orders of magnitude below that for L-Cth hydrolysis. A unique feature of S339A is the 340-nm absorbance observed upon reaction with L-Cth (Figure 4). The wild-type eCBL and S339A enzymes were incubated with 3 mM L-Cth (150 mol equiv) for 2 h, followed by dialysis to remove substrates and products. The enzymes were subsequently incubated with 20 mM pyruvate for 2 h, followed by dialysis to remove excess pyruvate, to return any pyridoxamine (PMP), produced by transamination of L-Cth, to the internal aldimine of PLP. Upon reaction of the wild-type enzyme with L-Cth the 424-nm peak, corresponding to the ketimine tautomer of the internal aldimine of the PLP cofactor, decreases in intensity, with a concomitant increase at 326 nm. In contrast, the 422-nm peak of S339A is shifted to 338 nm following reaction with L-Cth (Figure 4). Incubation with 20 mM pyruvate for 2 h, followed by dialysis, had no effect on the 424-nm absorbance of the wild-type enzyme, as the slight increase in absorbance observed is due to residual pyruvate. In contrast, incubation with pyruvate resulted in a 2.3-fold increase

dx.doi.org/10.1021/bi201090n | *Biochemistry* 2011, 50, 9876−9885

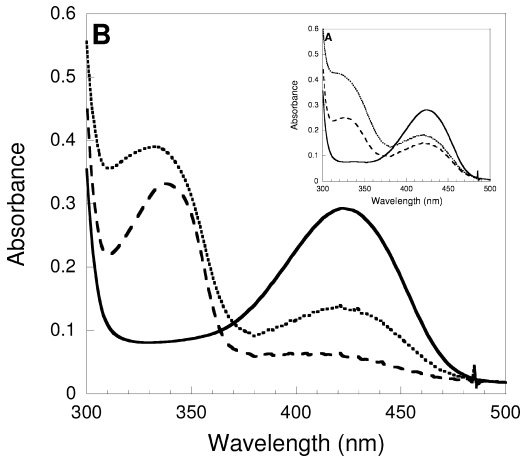

Figure 4. The effect of consecutive incubation with L-Cth and pyruvate on the PLP spectrum of (**A**) wild-type eCBL and (**B**) the S339A variant. The absorbance spectrum of the PLP cofactor of 20 μM enzyme was recorded before the addition of substrate (solid line), following a 2-h incubation with 3 mM L-Cth (dashed line) and following a 2-h incubation of the L-Cth-treated enzyme with 20 mM pyruvate (dotted line). The enzymes were dialyzed for one hour following both incubations to remove excess L-Cth and pyruvate.

in the intensity of the corresponding 422-nm band of S339A, suggesting that the PMP formed upon reaction with L-Cth reacted with the α-ketoacid pyruvate to produce alanine and regenerate the PLP form of the cofactor (Figure 4).

DISCUSSION

Cystathionine β-lyase is a member of the γ-subfamily of the large and diverse fold-type I class of PLP-dependent enzymes.[6] Crystal structures are available for 14 enzymes from the γ-subfamily, including plant and *E. coli* CBL and CGS, yeast and human CGL, and methionine γ-lyase (MGL), homocysteine γ-lyase (HGL), *O*-acetylhomoserine sulfhydrylase (OAHSS), and *O*-succinylhomoserine sulfhydrylase (OSHSS) from Trichomonads and diverse bacterial species.[4,7−9,16−25] Comparison of the amino-acid sequences and structures of these enzymes highlights their striking structural similarity and the conservation of key active-site residues. For example, of the 22 positions conserved between the 14 available γ-subfamily structures seven (corresponding to eCBL-Y56, R58, G86, D185, T209, K210, and R372) are involved in cofactor and/or substrate binding and positioning. In contrast, other active-site residues proposed to play a role in substrate binding or catalysis in eCBL, such as Y111, Y238, Y338, and S339, are less conserved between family members and may act as determinants of substrate or reaction specificity. Site-directed mutagenesis was employed to replace residues Y56, Y111, Y238 and Y338 with phenylalanine and S339 with alanine to probe the roles of the side-chain hydroxyl moiety of each. The structural similarity and subtle differences in active-site architecture between the enzymes of the γ-subfamily of fold-type I provides an interesting model system for the investigation of substrate and reaction specificity among enzymes dependent on the catalytically versatile PLP cofactor.

Residue Y338. The presence of a tyrosine residue at position 338 (of eCBL) is unique to bacterial CBL sequences. This residue is a valine in the three available MGL structures and in *A. thaliana* CBL (AtCBL) and is replaced by a glutamate in eCGS and both yeast and human CGL.[4,7−9,16−18,23,25] The observed change of less than 2-fold in the kinetic parameters of the Y338F variant (Tables 1 and 2) indicates that elimination of the hydrogen bond between the side chains of Y338 and K42 (Scheme 2), and ensuing increased conformational flexibility of Y338, does not substantially alter the hydrophobic packing interactions of the aromatic ring, which are proposed to play a role in substrate and inhibitor binding.[3,5,7] Interestingly, K42 is situated within a segment of eight amino acids in eCBL (residues 38−45), NtCGS, and MGL that is absent in eCGS, AtCBL, and CGL sequences. A role for F55 and Y338 of eCBL, and the corresponding E48 and E333 of yCGL and D45 and E325 of eCGS, as determinants of reaction specificity in the α,β versus α,γ-elimination of L-Cth of eCBL and yeast CGL (yCGL) has been suggested.[9] However, while these residues may contribute to regulation of reaction specificity, the near-native kinetic parameters of the eCBL-Y338F variant, in combination with the lack of change in reaction specificity in the eCBL (F55D, Y338E), eCGS (D45F, E325Y) and yCGL (E48F, E333Y) interconversion variants reported by Farsi et al., demonstrate that they must act in concert with other residues to modulate the chemistry of the PLP cofactor.[11]

Residues Y111 and Y238. The structure of the eCBL−AVG complex provides a useful model for the design of inhibitors and interpretation of binding interactions.[3] However, the binding mode observed for the distal portion of AVG may not be representative of the L-Cth substrate because the β,γ-unsaturated inhibitor lacks rotational freedom about this bond, a sulfur atom at the γ-position and the distal carboxylate group of the substrate (Scheme 1). Lodha et al. determined that the side chain of eCBL-R58 interacts with the distal carboxylate group of L-Cth, as the R58A substitution disparately increased the $K_m^{L\text{-}Cth}$ and K_i^{AVG} by 30- and 3-fold, respectively.[10] The side chain hydroxyl moieties of Y111 and Y238 are situated 2.8 and 4.2 Å, respectively, from the distal amino group of AVG (Scheme 2) and the latter interaction is enabled by a bridging water molecule.[3]

Residue Y238 is conserved in bacterial CBL sequences but is replaced by an asparagine residue in bacterial CGS and eukaryotic CGL, which also bind dicarboxylic substrates, and by isoleucine or leucine in MGL, the methionine substrate of which lacks a distal, hydrogen-bonding group. Comparison of the 15-fold increase in $K_m^{L\text{-}Cth}$ with the ∼2-fold increases in IC_{50}^{AVG} and K_i^{AVG}, for inhibition of eCBL-Y238F by AVG, and the K_m^{OAS} and $K_m^{L\text{-}Cys}$, for hydrolysis of OAS and L-Cys, respectively, indicates a role for this residue in binding to the distal carboxylate group of L-Cth, as this group is not present in AVG, L-Cys and OAS (Table 1). Similarly, the $K_m^{L\text{-}Cys}$, for the hydrolysis of L-Cys, of R58A is increased only 1.5-fold. The 23-fold increase in $K_m^{L\text{-}OAS}$ observed for R58A suggests that residue R58, which binds the distal carboxylate of L-Cth, may interact with the carbonyl oxygen of the acetate moiety of OAS.[10] The comparable, 2−3-fold, reductions in substrate inhibition by L-Cys observed for both Y238F and R58A (Figure 1B, Table 2) also indicate a common role for these residues in interacting with the distal portion of the L-Cth substrate, the binding site of which can be occupied by L-Cys.

Residue Y111 engages in a π-stacking interaction with the aromatic ring of the cofactor, an interaction common among fold-type I, PLP-dependent enzymes, as exemplified by W140 of *E. coli* AAT (eAAT) and H142 of *Rhodobacter capsulatus* 5-aminolevulinate synthase (ALAS).[26,27] Among the 14 structures of members of the γ-subfamily, a tyrosine is found in this position in 12 enzymes, including CGL, MGL and both plant

and bacterial CBL and CGS, while a phenylalanine is present in *Mycobacterium tuberculosis* OSHSS and *Thermus thermophilus* OAHSS.[19−21] Therefore, the presence of an aromatic ring that can engage in π-stacking with the cofactor, rather than the specific identity of this residue, is the common element shared by all members of the γ-subfamily for which structures are available. Although Y111 interacts with the distal amino group of AVG in the eCBL-AVG complex, removing the hydroxyl group of this residue increases the IC_{50}^{AVG} and $K_m^{L\text{-}Cth}$ by less than 2-fold and 3.6-fold, respectively (Table 1), suggesting that the crystal structure may differ from the binding mode of the L-Cth substrate and from the eCBL-AVG complex in solution. Alternatively, a water molecule may assume the role of the missing hydroxyl group of Y111 in the phenylalanine-replacement variant, thereby giving rise to the small changes observed in the kinetic parameters. Distinct features of the Y111F variant are the 7.5-fold decrease in $K_i^{L\text{-}Cys}$ for the α,β-elimination of L-Cys and the 250-fold difference between $k_{cat}/K_m^{L\text{-}Cth}$ values for the measurement of L-Cth hydrolysis with the DTNB and LDH assays, which monitor the production of L-Hcys and pyruvate, respectively. These results suggest that Y111 is an indirect determinant of substrate and reaction specificity, as although removal of the hydroxyl group of this residue alters the K_m of L-Cth, L-Cys and L-OAS by only 2−6-fold, it enables a conformational change in the active site that allows inhibition of the enzyme by DTNB and facilitates the binding of a second molecule of L-Cys, to inhibit the release of pyruvate in favor of lanthionine formation (Tables 1 and 2, Figures 1 and 5). The production of lanthionine from L-Cys has also been reported for human CGL.[28] The decrease of only ∼2-fold in the k_{cat} of the L-Cth hydrolysis reaction (Table 1), in combination with the similarity in the $k_{cat}/K_m^{L\text{-}Cth}$ versus pH profiles of wild-type eCBL and the Y111F variant (Figure 2C, Table 3), demonstrate that Y111 does not participate in proton transfer from the α-amino group of the substrate to the aminoacrylate product as previously suggested.[3,7]

Residues Y56 and S339. The conservation of eCBL-Y56 in all members of the γ-subfamily, as well as many enzymes of the broader fold-type I family suggests the involvement of this residue in a process fundamental to the enzymes of this structural class.[29−31] Conversely, the presence of a serine residue at the position corresponding to eCBL-S339 is restricted to 12 of the 14 structures for members of the γ-subfamily, suggesting that this residue may act as a determinant of specificity. The side-chain hydroxyl groups of residues Y56 and S339 are within hydrogen-bonding distance, 2.9 and 2.7 Å, respectively, of the ε-amino group of K210 in the structure of the eCBL-AVG complex (Scheme 2).[3] Tethering of the catalytic base in this manner is likely required to enforce reaction specificity, as protonation of position C4′ of the cofactor could result in γ-elimination/replacement or trans-amination, as observed for eCGS and eAAT, respectively.[3,13,32] Residues Y56 and S339 are restrained by direct and indirect, respectively, interactions with the cofactor. A 2.6-Å hydrogen bond to OP2 tethers Y56 to the phosphate moiety, while S339 is positioned by the adjacent W340, which interacts with O3′ of the cofactor (Scheme 2). Residue W340, conserved in bacterial CBL, is replaced by leucine in bacterial CGS and fungal and animal CGL sequences. Interestingly, substitution of either Y338 or W340 with phenylalanine results in a 2−3-fold increase in the k_{cat} for L-Cth hydrolysis, suggesting that the interactions formed by these residues, which flank S339, are not essential for the positioning of the latter (Scheme 2, Table 1).[10]

The minor, 6-fold decrease in k_{cat} observed for the phenylalanine substitution variant of eCBL-Y56 demonstrates that this residue does not participate in catalysis. The similar 21 and 50-fold increases in the $K_m^{L\text{-}Cth}$ and K_i^{AVG} values, respectively, of Y56F (Table 1) suggest that Y56 interacts with the distal amino group that is common to L-Cth and AVG (Scheme 1). However, this contradicts the evidence of the eCBL−AVG structure in which the distal amino group of AVG is 2.8 and 6.5 Å from the side-chain hydroxyl groups of Y111 and Y56, respectively (Scheme 2).[3] Site-directed replacement of the residue corresponding to Y56 of eCBL in other fold-type-I enzymes has produced a similar effect as observed for eCBL-Y56F and a common role in binding the phosphate group of PLP, thereby preventing cofactor dissociation, has been reported for Y70 of *E. coli* AAT (eAAT), Y64 of *Treponema denticola* cystalysin (Td-Cys), and Y121 of murine erythroid ALAS (meALAS).[29−31,33,34] Interestingly, the K_d^{PLP} and K_m for glycine of the corresponding Y121F variant of meALAS are increased 15 and 34-fold, while the k_{cat} is decreased by only 3-fold.[31] The glycine substrate of meALAS cannot form a hydrogen bond with the side-chain hydroxyl moiety of Y121. Therefore, Tan et al. proposed that the observed reduction in K_m is due to the decrease in K_d^{PLP}.[31] This presents an alternative explanation for the observed 22- and 50-fold increases in the $K_m^{L\text{-}Cth}$ and K_i^{AVG} values of eCBL-Y56F (Table 1) that does not require the formation of a hydrogen bond between the hydroxyl moiety of Y56 and the distal amino group of L-Cth or AVG. Additionally, the increased flexibility in positioning of the phenylalanine side chain of Y56F, due to loss of the restraining link to the phosphate moiety of the cofactor, may allow this residue to move toward the entrance of the active site, thereby impeding substrate binding. In contrast with eCBL-Y56F, eAAT-Y70F, Td-Cys-Y64F, and meALAS-Y121F, the k_{cat} of the corresponding Y71F variant of tyrosine phenol−lyase (TPL) for the substrate tyrosine is reduced $>10^5$-fold and the formation of a stable quinonoid intermediate is observed. This demonstrates that Y71 of TPL is unique as it participates in β-elimination, via activation of the C1−Cβ bond, by removal of the side-chain hydroxyl proton of the tyrosine substrate and subsequent protonation at position C1.[35] The Y56F substitution is unique among the variants investigated in this study in that it is the only one to exhibit a change in the activity versus pH profile (Figure 2). A similar increase of ∼0.7 pH units in the pK_a value of the acidic limb (pK_{a1}) of the $k_{cat}/K_m^{L\text{-}Cth}$ versus pH profile is observed for both R58K and Y56F (Table 3).[10] Vacca et al. reported a similar narrowing of the specific activity versus pH profile for the corresponding R292K variant of eAAT and proposed that the change may be due to deprotonation of K292, as the pK_a of lysine is lower than that of arginine.[36] However, a similar mechanism is unlikely in the case of the eCBL−R58K or Y56F variants, as both residues interact with the phosphate moiety of the PLP cofactor. The increase in pK_{a1} observed for both R58K and Y56F is likely an indirect effect due to a change in the conformation or charge distribution of the active site resulting from a shift in the positioning of the negatively charged phosphate group of the cofactor, which is tethered in the eCBL active site by seven hydrogen bonds, including one to Y56 and a pair to R58 (Scheme 2). Alternatively, although the titrating group corresponding to pK_{a1} has not been identified, removing a hydrogen bond from the phosphate moiety of the PLP cofactor could raise the pK_a of the phosphate group itself or the effect could be transmitted to the aldimine nitrogen.

In contrast with the minor effect of Y56F on k_{cat}, removal of the hydroxyl group of S339, by the S339A substitution, reduces the k_{cat} for L-Cth hydrolysis by 5600-fold, while increasing $K_m^{L\text{-}Cth}$ by only 2-fold (Table 1), a result in keeping with a primary role for this residue in tethering the catalytic base, K210. The 340-nm peak observed upon reaction of eCBL−S339A with 3 mM L-Cth, and the reduction of this absorbance upon subsequent incubation with pyruvate, is unique to this enzyme variant and suggestive of pyridoximine (PMP) formation, resulting from protonation of C4′ (Figure 4). This indicates that although the ε-amino group of K210 forms hydrogen bonds to the side chains of both Y56 and S339, only the latter acts as a determinant of reaction specificity, a conclusion consistent with the conservation of residues corresponding to Y56 in the broader fold-type I of PLP-dependent enzymes and S339 only in a subset of the γ-subfamily. Similar interactions occur between the ε-amino group of the catalytic base, K258, and residues Y70 and G38 of the extensively studied and archetypical PLP-dependent enzyme eAAT. Interestingly, the 2011 report by Griswold et al. of the structure of the eAAT external aldimine of deazaPLP in complex with aspartate was the first to observe the G38−K258 hydrogen bond because steric hindrance by the α-methyl moiety of the α-methylaspartate substrate analogue, employed in previous eAAT structural studies, precluded the formation of this interaction.[37,38] However, the function of residue G38 in tethering or guiding the ε-amino group of eAAT-K258 has not yet been explored. Therefore, the evidence presented here, indicating a role for eCBL-S339 in restraining and orienting the catalytic base, is the first report of a residue in this position modulating the reaction specificity of a PLP-dependent enzyme of the large and diverse fold type I family.

CONCLUSIONS

Cystathionine β-lyase is an attractive target for the development of novel antimicrobial compounds because it is unique to bacteria and plants. This study has identified Y238, a residue conserved in bacterial CBL sequences, as a determinant of substrate specificity as it interacts with the distal carboxylate group of the L-Cth substrate. The identity, position, and flexibility of active-site residues are key determinants of both the substrate and reaction specificity, particularly for enzymes dependent on the catalytically versatile PLP cofactor. For example, residue eCBL-S339, which is conserved among many members of the γ-subfamily, is identified in this study as a determinant of reaction specificity. In contrast, while the ability of an aromatic residue, corresponding to eCBL−Y111, to engage in a π-stacking interaction with the cofactor is a common feature of fold-type-I enzymes, the specific identity of this residue varies and substitution of Y111 with phenylalanine only marginally impacts the physiological L-Cth hydrolysis reaction. However, the enhanced L-Cys substrate inhibition of Y111F suggests an indirect role, likely via modulation of active-site architecture, for this residue in reaction specificity. The information resulting from this study will guide the design of inhibitors specific for bacterial CBL, a challenging target given the structural similarity of the γ-subfamily enzymes, as well as facilitate protein engineering studies aimed at modifying the substrate and reaction specificity of PLP-dependent enzymes.

AUTHOR INFORMATION

Corresponding Author

*Tel: (613) 520-2600. Fax: (613) 520-3539. E-mail: susan_aitken@carleton.ca.

Funding

This work was funded by the Natural Sciences and Engineering Research Council of Canada.

ACKNOWLEDGMENTS

We thank the reviewers of this paper for their insightful comments and suggestions and Heidi Los and Navya Kalidindi for their technical assistance in protein purification.

REFERENCES

(1) Aitken, S. M., and Kirsch, J. F. (2005) The enzymology of cystathionine biosynthesis: strategies for the control of substrate and reaction specificity. *Arch. Biochem. Biophys. 433*, 166−175.

(2) Aitken, S. M., Lodha, P. L., and Morneau, D. J. K. (2011) *The enzymes of the transsulfuration pathways: active-site characterizations*, in press.

(3) Clausen, T., Huber, R., Messerschmidt, A., Pohlenz, H. D., and Laber, B. (1997) Slow-binding inhibition of Escherichia coli cystathionine β-lyase by L-aminoethoxyvinylglycine: a kinetic and X-ray study. *Biochemistry 36*, 12633−12643.

(4) Clausen, T., Huber, R., Prade, L., Wahl, M. C., and Messerschmidt, A. (1998) Crystal structure of Escherichia coli cystathionine gamma-synthase at 1.5 A resolution. *EMBO J. 17*, 6827−6838.

(5) Ejim, L. J., Blanchard, J. E., Koteva, K. P., Sumerfield, R., Elowe, N. H., Chechetto, J. D., Brown, E. D., Junop, M. S., and Wright, G. D. (2007) Inhibitors of bacterial cystathionine β-lyase: leads for new antimicrobial agents and probes of enzyme structure and function. *J. Med. Chem. 50*, 755−764.

(6) Percudani, R., and Peracchi, A. (2009) The B6 database: a tool for the description and classification of vitamin B6 dependent enzymatic activities and of the corresponding protein families. *BMC Bioinf. 10*, 273−281.

(7) Clausen, T., Huber, R., Laber, R., Pohlenz, H. D., and Messerschmidt, A. (1996) Crystal structure of the pyridoxal-5′-phosphate dependent cystathionine β-lyase from Escherichia coli at 1.83 Å. *J. Mol. Biol. 262*, 202−224.

(8) Goodall, G., Mottram, J. C., Coombs, G. H., Lapthorn, A. J. (2001) Methionine γ-lyase from *Trichomonas vaginales,* Unpublished crystal structure. PDB accession: 1E5F.

(9) Messerschmidt, A., Worbs, M., Steegborn, C., Wahl, M. C., Huber, R., Laber, B., and Clausen, T. (2003) Determinants of enzymatic specificity in the Cys-Met-metabolism PLP-dependent enzymes family: crystal structure of cystathionine γ-lyase from yeast and intrafamiliar structure comparison. *Biol. Chem. 384*, 373−386.

(10) Lodha, P. H., Jaworski, A. F., and Aitken, S. M. (2010) Characterization of site-directed mutants of residues R58, R59, D116, W340 and R372 in the active site of *E. coli* cystathionine β-lyase. *Protein Sci. 19*, 383−391.

(11) Farsi, A., Lodha, P. H., Skanes, J. E., Los, H., Kalidindi, N., and Aitken, S. M. (2009) Inter-conversion of a Pair of Active-Site Residues in *E. coli* Cystathionine γ-Synthase, *E. coli* Cystathionine β-Lyase and *S. cerevisiae* Cystathionine γ-Lyase and Development of Tools for the Investigation of Mechanism and Reaction Specificity. *Biochem. Cell Biol. 87*, 445−457.

(12) Ellman, G. L. (1959) Tissue sulfhydryl groups. *Arch. Biochem. Biophys. 82*, 70−77.

(13) Aitken, S. M., Kim, D. H., and Kirsch, J. F. (2003) *Escherichia coli* cystathionine γ-synthase does not obey ping-pong kinetics. Novel continuous assays for the elimination and substitution reactions. *Biochemistry 42*, 11297−11306.

(14) Peracchi, A., Bettati, S., Mozzarelli, A., Rossi, G. L., Miles, E. W., and Dunn, M. F. (1996) Allosteric regulation of tryptophan synthase:

effects of pH, temperature, and α-subunit ligands on the equilibrium distribution of pyridoxal 5′-phosphate-L-serine intermediates. *Biochemistry 35*, 1872−1880.
(15) Jhee, K. H., McPhie, P., and Miles, E. W. (2000) Domain architecture of the heme-independent yeast cystathionine β-synthase provides insights into mechanisms of catalysis and regulation. *Biochemistry 39*, 10548−10556.
(16) Allen, T. W., Sridhar, V., Prasad, S. G., Han, Q., Xu, M., Tan, Y., Hoffman, R. M., Ramaswamy, S. (2009) Methionine γ-lyase from *Trichomonas vaginales,* Unpublished crystal structure. PDB accession: 1PFF.
(17) Allen, T. W., Sridhar, V., Prasad, S. G., Han, Q., Xu, M., Tan, Y., Hoffman, R. M., Ramaswamy, S. (2009). Crystal Structure of L-methionine α,γ-lyase, Unpublished crystal structure. PDB accession: 1PG8.
(18) Breitinger, U., Clausen, T., Ehlert, S., Huber, R., Laber, B., Schmidt, F., Pohl, E., and Messerschmidt, A. (2001) The three-dimensional structure of cystathionine β-lyase from Arabidopsis and its substrate specificity. *Plant Physiol. 126*, 631−642.
(19) Edwards, T. E., Gardberg, A. S., Sankaran. B. (2010) Crystal structure of *O*-succinylhomoserine sulfhydrylase from Mycobacterium tuberculosis covalently bound to pyridoxal-5-phosphate, Unpublished crystal structure. PDB accession: 3NDN.
(20) Imigawa, T., Utsunomiya, H., Agari, Y., Satoh, S., Tsuge, H. (2009) The crystal structure of *O*-acetylhomoserine-2 from *Thermus thermophilus* HB8. Unpublished crystal structure. PDB accession: 2CB1.
(21) Imagawa, T., Kousumi, Y., Tsuge, H., Utsunomiya, H., Ebihara, A., Nakagawa, N., Yokoyama, S., Kuramitsu, S. (2009) Crystal structure of o-acetyl homoserine sulfhydrylase from Thermus thermophilus HB8Unpublished crystal structure. PDB accession: 2CTZ.
(22) Ngo, H. P. T., Kim, J. K., Kim, H. S., Jung, J. H., Ahn, Y. J., Kim, J. G., Lee, B. M., Kang, H. W., Kang, L. W. (2009) Crystal structure of XometC, a cystathionine γ-lyase-like protein from *Xanthomonas oryzae* pv.*oryzae*. Unpublished crystal structure. PDB accession: 3E6G.
(23) Nikulin, A., Revtovich, S., Morozova, E., Nevskaya, N., Nikonov, S., Garber, M., and Demidkina, T. (2008) High-resolution structure of methionine γ-lyase from *Citrobacter freundii*. *Acta Crystalogr., Sect. D 64*, 211−218.
(24) Steegborn., C., Messerschmidt, A., Laber, B., Streber, W., Huber, R., and Clausen, T. (1999) The crystal structure of cystathionine γ-synthase from Nicotiana tabacum reveals its substrate and reaction specificity. *J. Mol. Biol. 290*, 983−996.
(25) Sun, Q., Collins, R., Huang, S., Holmberg-Schiavone, L., Anand, G. S., Tan, C.-H., van-den-Berg, S., Deng, L.-W., Moore, P. K., Karlberg, T., and Sivaraman, J. (2009) Structural basis for the inhibition mechanism of human cystathionine γ-lyase, an enzyme responsible for the production of H_2S. *J. Biol. Chem. 284*, 3076−3085.
(26) Hayashi, H., Inoue, Y., Kuramitsu, S., Morino, Y., and Kagamiyama, H. (1990) Effects of replacement of tryptophan-140 by phenylalanine or glycine on the function of escherichia coli aspartate aminotransferase. *Biochem. Biophys. Res. Commun. 167*, 407−412.
(27) Astner, I., Schulze, J. O., van den Heuvel, J., Jahn, D., Schubert, W. D., and Heinz, D. W. (2005) Crystal structure of 5-aminolevulinate synthase, the first enzyme of heme biosynthesis, and its link to XLSA in humans. *EMBO J. 24*, 3166−3177.
(28) Chiku, T., Padovani, D., Zhu, W., Singh, S., Vitvitsky, V., and Banerjee, R. (2009) H_2S biogenesis by human cystathionine gamma-lyase leads to the novel sulfur metabolites lanthionine and homolanthionine and is responsive to the grade of hyperhomocysteinemia. *J. Biol. Chem. 284*, 11601−11612.
(29) Cellini, B., Bertoldi, M., Montioli, R., and Voltattorni, C. B. (2005) Probing the role of Tyr64 of Treponema denticola cystalysin by site-directed mutagenesis and kinetic studies. *Biochemistry 44*, 13970−13980.
(30) Toney, M. D., and Kirsch, J. F. (1991) Tyrosine 70 fine-tunes the catalytic efficiency of aspartate aminotransferase. *Biochemistry 30*, 7456−7461.
(31) Tan, D., Barber, M. J., and Ferreira, G. C. (1998) The role of tyrosine 121 in cofactor binding of 5-aminolevulinate synthase. *Protein Sci. 7*, 1208−1213.
(32) Eliot, A. C., and Kirsch, J. F. (2004) Pyridoxal phosphate enzymes: mechanistic, structural, and evolutionary considerations. *Annu. Rev. Biochem. 73*, 383−415.
(33) Toney, M. D., and Kirsch, J. F. (1991) Kinetics and equilibria for the reactions of coenzymes with wild type and the Y70F mutant of Escherichia coli aspartate aminotransferase. *Biochemistry 30*, 7461−7466.
(34) Krupka, H. L., Huber, R., Holt, S. C., and Clausen, T. (2000) Crystal structure of cystalysin from *Treponema denticola*: A pyridoxal 5′-phosphate-dependent protein acting as a haemolytic enzyme. *EMBO J. 19*, 3168−3178.
(35) Chen, H. Y., Demidkina, T. V., and Phillips, R. S. (1995) Site-directed mutagenesis of tyrosine-71 to phenylalanine in *Citrobacter freudnii* tyrosine phenol-lyase: evidence for dual roles of tyrosine-71 as a general acid catalyst in the reaction mechanism and in cofactor binding. *Biochemistry 34*, 12276−12283.
(36) Vacca, R. A., Giannattasio, S., Graber, R., Sandmeier, E., Marra, E., and Christen, P. (1997) Active-site Arg-Lys substitutions alter reaction and substrate specificity of aspartate aminotransferase. *J. Biol. Chem. 272*, 21932−21937.
(37) Okamoto, A., Higuchi, T., Hirotsu, K., Kuramitsu, S., and Kagamiyama, H. (1994) X-ray crystallographic study of pyridoxal 5′-phosphate-type aspartate aminotransferases from Escherichia coli in open and closed form. *J. Biochem. 116*, 95−107.
(38) Griswold, W. R., Fisher, A. J., and Toney, M. D. (2011) Crystal structures of aspartate aminotransferase reconstituted with 1-deazapyridoxal 5′-phosphate: internal aldimine and stable L-Aspartate external aldimine. *Biochemistry 50*, 5918−5924.